On the influence of elastic strain on the accommodation of carbon atoms into substitutional sites in strained Si:C layers grown on Si substrates

Nikolay Cherkashin, Martin Hÿtch, Florent Houdellier, Florian Hüe, Vincent Paillard, Alain Claverie, A. Gouyé, O. Kermarrec, Denis Rouchon, M. Burdin, et al.

On the influence of elastic strain on the accommodation of carbon atoms into substitutional sites in strained Si:C layers grown on Si substrates

N. Cherkashin, M. J. Hÿtch, F. Houdellier, F. Hüe, V Paillard, A. Claverie, A. Gouyé, O. Kermarrec, D. Rouchon, M. Burdin, and P. Holliger

Citation: Appl. Phys. Lett. **94**, 141910 (2009); doi: 10.1063/1.3116648
View online: https://doi.org/10.1063/1.3116648
View Table of Contents: http://aip.scitation.org/toc/apl/94/14
Published by the American Institute of Physics

On the influence of elastic strain on the accommodation of carbon atoms into substitutional sites in strained Si:C layers grown on Si substrates

N. Cherkashin,[1,a)] M. J. Hÿtch,[1] F. Houdellier,[1] F. Hüe,[1] V Paillard,[1] A. Claverie,[1] A. Gouyé,[2] O. Kermarrec,[2] D. Rouchon,[3] M. Burdin,[3] and P. Holliger[3]
[1]*Groupe nMat, CEMES-CNRS, 29 rue J. Marvig, 31055 Toulouse, France*
[2]*STMicroelectronics, 850 rue Jean Monnet, 38926 Crolles, France*
[3]*CEA-LETI, Minatec, 17 rue des Martyrs, 38054 Grenoble, France*

(Received 11 February 2009; accepted 19 March 2009; published online 9 April 2009)

Measurements of strain and composition are reported in tensile strained 10- and 30-nm-thick Si:C layers grown by chemical vapor deposition on a Si (001) substrate. Total carbon concentration varies from 0.62% to 1.97%. Strain measurements were realized by high-resolution x-ray diffraction, convergent-beam electron diffraction, and geometric phase analysis of high-resolution transmission electron microscopy cross-sectional images. Raman spectroscopy was used for the deduction of the substitutional concentration. We demonstrate that in addition to the growth conditions, strain accumulating during deposition, thus depending on a layer thickness, has an influence on the final substitutional carbon composition within a strained Si:C layer. © *2009 American Institute of Physics*. [DOI: 10.1063/1.3116648]

Strain engineering is currently used in most advanced transistors to increase carrier mobility in active regions of devices. For *p*-type devices, selectively etched regions containing $Si_{1-x}Ge_x$ alloys can be used to compressively strain the silicon lattice in the channel region, thus providing enhanced hole mobility.[1] For *n*-type devices, silicon needs to be tensile strained to increase electron mobility and a possible route is to use regions of carbon-doped silicon (*s*-Si:C).[2] For a $Si_{1-y}C_y$ alloy with carbon atoms incorporated substitutionally, the lattice parameter is reduced with respect to silicon. However, due to the extremely low solid solubility of C in Si under equilibrium conditions,[3] the incorporation of C atoms into substitutional sites is nontrivial and can only be obtained by using far from equilibrium growth conditions.[4–7] So far, substitutional carbon compositions C^{sub} of a maximum of about 1% have been obtained within typical 100-nm-thick *s*-Si:C layers grown by different techniques and these are for total carbon concentrations which usually double.[4–7]

It is generally believed that the relatively large concentrations of C^{sub} obtained are due to some sort of increase in the solid solubility of carbon due to kinetics factors, under the specific growth conditions used. In this work, we will show that in addition, the elastic energy accumulated in the layers during growth governs the maximum attainable substitutional composition C^{sub}. Hence, the concentration also depends on the total thickness of the grown layer. To demonstrate this, we have used a wide range of different experimental techniques aimed at dosing C in its different states in the crystal.

Strained 10- and 30-nm-thick *s*-Si:C films were grown on 8-in. Si (001) substrates by chemical vapor deposition in an industrial "reduced pressure" (ASM Epsilon®) reactor. Films were grown at 550 °C with $SiCH_6$ mass flow ratios (MFRs) of 2.5, 4.9, and 7.4×10^{-4} and at 600 °C with an MFR of 4.2×10^{-4}. The total carbon concentration C^{total}, incorporated within these Si:C films containing substitutional C^{sub} and interstitial C^{int} carbon concentrations, was measured by secondary ion mass spectroscopy to be 0.62%, 1.16%, 1.50% (550 °C growth temperature), and 1.97% (600 °C growth temperature) on multilayer samples grown under exactly the same conditions.

High-resolution x-ray diffraction (HR-XRD) and transmission electron microscopy (TEM) techniques were used to obtain independent measurements of the out-of-plane strain of the *s*-Si:C layers with respect to Si, defined as $\varepsilon_{zz}^{Si}\equiv(c-a^{Si})/a^{Si}$, where a^{Si} is the bulk lattice constant of Si (0.543 nm) and c, the measured lattice constant of *s*-Si:C in the z =[001] growth direction. HR-XRD was performed on a Philips X'Pert MRD system at a Cu $K\alpha1$ wavelength of 1.5406 Å using a probe size of approximately 1 mm^2. The out-of-plane strain was deduced from the relative shift of the (004) peaks.

Specimens were prepared for TEM by tripod polishing and argon ion-beam thinning (Gatan PIPS) to about 200-nm-thickness for convergent-beam electron diffraction (CBED) measurements and 30-nm-thickness for HRTEM observations. Both techniques were performed on the SACTEM-Toulouse, a Tecnai F20 (FEI) operating at 200 kV, equipped with an imaging aberration corrector (CEOS) and imaging filter (Gatan GIF Tridiem). The probe size for CBED measurements was 2 nm. Strain was determined by comparing the broadening and displacements of higher-order Laue zone (HOLZ) lines with finite element modeling and dynamical elastic scattering simulations.[8]

Geometric phase analysis (GPA) of the HRTEM images[9] was used to directly map the distribution of ε_{zz}^{Si}, within the whole structures with nanometer resolution and high precision of 0.1%.[10,11] Image analysis was carried out using GPA Phase 2.0 (HREM Research, Inc.) a plug-in for the software package DigitalMicrograph (Gatan). Thin film relaxation was corrected for by assuming that strains were fully relaxed in the viewing direction.[12]

The in-plane strain relative to the bulk lattice parameter of Si:C ε_{xx}, which is actually the negative misfit $-f$ was then

a)Electronic mail: nikolay@cemes.fr.

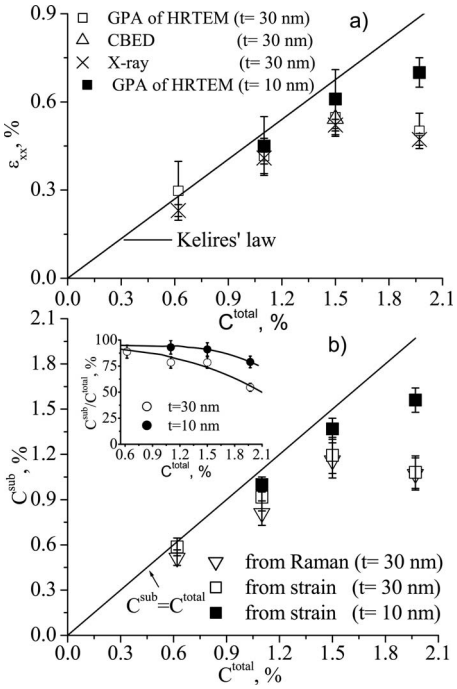

FIG. 1. Strain measurements in *s*-Si:C layers grown pseudomorphically on Si (001). (a) In-plane strain ε_{xx} calculated from the experimental results obtained by different techniques and predicted values for fully substitutional $Si_{1-x}C_x$ alloys (Ref. 13). (b) C^{sub} obtained by Raman spectroscopy (triangles) and deduced from strain measurements (squares). The ratio C^{sub}/C^{total} is shown in the inset.

calculated from the measured ε_{zz}^{Si} using the following expression:

$$\varepsilon_{xx} = -f \equiv \frac{a^{\text{in-plane}} - a^{\text{Si:C}}}{a^{\text{Si:C}}} = -\varepsilon_{zz}^{\text{Si}}\left(2\frac{C_{12}^{\text{Si:C}}}{C_{11}^{\text{Si:C}}} + \varepsilon_{zz}^{\text{Si}} + 1\right)^{-1}, \tag{1}$$

where $C_{12}^{Si:C}$ and $C_{11}^{Si:C}$ are elastic constants and $a^{Si:C}$ is the lattice constant of relaxed Si:C, $a^{in\text{-}plane}$ is the in-plane lattice constant of *s*-Si:C equal a^{Si} in our case. The elastic constants were calculated using the linear interpolation between elastic constants of β-SiC (Refs. 13 and 14) and Si.

The results for the in-plane strain are plotted in Fig. 1(a) as a function of C^{total}. Their good overall agreement is proof of the reliability of the different techniques, and also of the excellent strain homogeneity in these layers given the wide range of probe sizes of the different techniques. For the 10-nm-thick layers ε_{xx} increases continuously with C^{total}, as expected. While for the 30-nm-thick layers ε_{xx} follows a similar trend up to $C^{total}=1.5\%$, for $C^{total}=1.97\%$, the strain is surprisingly even less than for $C^{total}=1.5\%$. For comparison, we have also plotted in Fig. 1(a) the predicted lattice parameters given by Kelires[15] for fully substitutional $Si_{1-x}C_x$ alloys (which deviate significantly from Vergard's law) $a(x)=a_{Si}-0.24239x+0.05705x^2$. Our experimental results are well-described by these predictions for C^{total} up to 1%, but then tail off. The results suggest that the carbon is indeed not fully substitutional.

For more direct information concerning the substitutional carbon concentration C^{sub}, we have performed UV Raman spectroscopy using an excitation source of 363.8 nm (penetration depth less than 15 nm). The shift $\Delta\omega$ was measured between the positions of the peaks associated with the Si–Si vibration modes in the 30-nm-thick *s*-$Si_{1-y}C_y$ layers and in the Si substrate. Using the values of ε_{xx} determined by XRD and TEM results, the C^{sub} within the *s*-Si:C layers can be deduced from the relation $\Delta\omega=+210\times C^{sub}-780\times\varepsilon_{xx}$.[16]

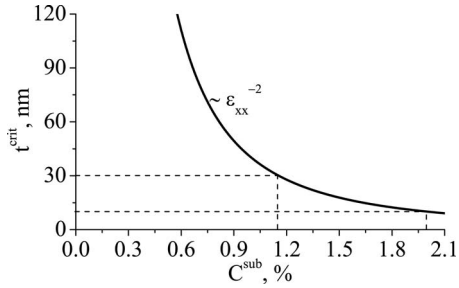

FIG. 2. Critical layer thickness t^{crit} as a function of C^{sub} in *s*-Si:C layers.

The results of the C^{sub} as a function of C^{total} obtained from Raman spectroscopy for the 30-nm-thick layers are plotted in Fig. 1(b) (open triangles). For consistency, the results of the C^{sub} as a function of C^{total} deduced from the strain measurements are also shown in Fig. 1(b) (open squares). It can be seen that they are in good agreement with the Raman spectroscopy results. Consequently, the results of the C^{sub} as a function of C^{total} deduced from the strain measurements for the 10-nm-thick layers are also expected to be close to reality [Fig. 1(b), solid squares]. For both layer thicknesses, the C^{sub} tails off with increasing C^{total} [see inset in Fig. 1(b)]. For 10-nm-thick layers, the ratio C^{sub}/C^{tot} dips below 100% from the concentration of $C^{total}=0.97\%$ onwards. The effect is even more pronounced for the 30- nm-thick layers. As more carbon atoms are incorporated in the layers, a larger fraction of them tends to occupy nonsubstitutional sites. Indeed for the highest concentration of 1.97% C^{total}, only 50% of the carbon is on substitutional sites.

GPA shows that the strain is homogeneous in the layers from the substrate to the surface. Since the ratio C^{sub}/C^{total} decreases during the growth of the layer it requires that a fraction of carbon atoms initially sitting on substitutional sites is ejected from these sites as the growth proceeds. The ratio C^{sub}/C^{total} is therefore controlled by the elastic energy stored in these layers.

The elastic energy of a *t*-thick *s*-Si:C layer is given in the isotropic elasticity approximation[17] by

$$E_{el} = \frac{2G(1+\nu)}{1-\nu}\cdot t\varepsilon_{xx}^2, \tag{2}$$

where G is shear modulus and ν is Poisson ratio of the layer material. The elastic properties of *s*-Si:C layers are close to that of pure Si, since only a small concentration of C atoms is diluted within Si matrix. Thus, approximately similar critical layer thickness t^{crit} exists for a tensile *s*-Si:C/Si layer, as it exists for a tensile *s*-Si/(relaxed $Si_{1-x}Ge_x$) layer with the same in-plane strain.

The latter condition is satisfied between *s*-$Si_{0.99}C_{0.01}$/Si and *s*-Si/$Si_{0.883}Ge_{0.117}$ layers. The t^{crit} of a *s*-Si/$Si_{0.8}Ge_{0.2}$ layer is about 14 nm.[18] Using these data, the dependence of t^{crit} of a tensile *s*-$Si_{1-y}C_y$/Si layer on the C^{sub} was calculated (Fig. 2). It follows that the deposited 30 nm layer thickness is well below an expected t^{crit} for $C^{sub}=C^{total}=0.62\%$ and it exceeds the t^{crit} for the C^{sub} higher than 1.15%. For $C^{sub}=C^{total}\leq 1.97\%$ the deposited 10 nm layer thickness is close to an expected t^{crit}.

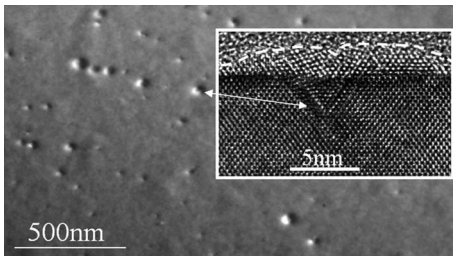

FIG. 3. Weak-beam dark-field $(g,2g)$ PV (001) image taken with $g=220$ showing the pyramidlike defects. CS (110) HRTEM image of a 3D pyramidlike defect is shown in inset.

Since no misfit dislocations associated with the strain relaxation are observed here or elsewhere,[3–7] the observed transformation of substitutional carbon atoms into interstitials during layer deposition seems to be the mechanism for strain relaxation. These interstitials can further precipitate in the form of three-dimensional (3D) pyramidal defects (Fig. 3), which are found in all the *s*-Si:C layers containing 1.5% of carbon or more. Defects have 4{111} sides and a bubble prominent at about 3–4 nm distance above the surface. Weak-beam dark-field imaging shows that in the 30-nm-thick samples, these defects appear at approximately 10–15 nm from the *s*-Si:C/Si interface. Their size (base width of about 20–25 nm) appears to be independent of the C^{total}, while their density increases from 1.2×10^{9} to 3×10^{9} cm^{-2}, as the C^{total} increases from 1.5% to 1.97%. In the respective 10-nm-thick samples, their density increases from 5×10^{8} to 1×10^{10} cm^{-2} but they are much smaller (base width of 4–5 nm).

An upper estimate of the amount of carbon that could be contained in these defects can be obtained by assuming an atomic density of carbon in their interior of 1.76×10^{23} cm^{-3}. The volume fraction occupied by the defects between the 10- and 30-nm-thick layers with $C^{total}=1.97\%$, taking into account the defect shape, size, and density, is approximately 0.09%–0.13% and 0.15%–0.25%, respectively, which results in overall carbon concentrations of 0.3%–0.4% and 0.6%–0.9%, respectively. In reality, the amount of carbon that can be incorporated in these defects will be less but the values are consistent with the concentrations of carbon interstitials that can be calculated from the graph in Fig. 1(b), i.e., $C^{int}=0.4\%$ and 0.9% in the 10- and 30-nm-thick samples, respectively. However, there is no evidence from the analysis of HRTEM images that these pyramidal defects contribute directly to relaxation of strain in the layers.

It was experimentally justified that the C^{sub} within a Si:C alloy can be correctly deduced from the Kelires' law. For a given C^{total}, the increase of a *s*-Si:C layer thickness results in the increase in its elastic energy. The overcoming of its t^{crit} gives rise to a partial layer strain relaxation through the transformation of substitutional carbon atoms into interstitials with their further precipitation in form of 3D pyramidlike defects.

This work was partially supported by the European Commission through the PullNano (Pulling the limits of nanoCMOS electronics, Contract No. IST-026828).

[1] M. Bohr, Intel's 90 nm Logic Technology Using Strained Silicon Transistors, INTEL Presentations, 2003, www.intel.com.
[2] K. Brunner, K. Eberl, and W. Winter, Phys. Rev. Lett. **76**, 303 (1996).
[3] R. W. Olesinski and G. J. Abbaschian, Bull. Alloy Phase Diagrams **5**, 486 (1984).
[4] S. S. Iyer, K. Eberl, M. S. Goorsky, F. K. Legoues, J. C. Tsang, and F. Cardone, Appl. Phys. Lett. **60**, 356 (1992).
[5] L. Simon, L. Kubler, J. L. Bischoff, D. Bolmont, J. Fauré, A. Claverie, and J. L. Balladore, Phys. Rev. B **54**, 10559 (1996).
[6] J. M. Hartmann, T. Ernst, V. Loup, F. Ducroquet, G. Rolland, D. Lafond, P. Holliger, F. Laugier, M. N. Séméria, and S. Deleonibus, J. Appl. Phys. **92**, 2368 (2002).
[7] V. LeThanh, C. Calmes, Y. Zheng, and D. Bouchier, Appl. Phys. Lett. **80**, 43 (2002).
[8] F. Houdellier, C. Roucau, L. Clément, J. L. Rouvière, and M. J. Casanove, Ultramicroscopy **106**, 951 (2006).
[9] M. J. Hytch, E. Snoeck, and R. Kilaas, Ultramicroscopy **74**, 131 (1998).
[10] N. Cherkashin, M. J. Hÿtch, E. Snoeck, F. Hüe, J. M. Hartmann, Y. Bogumilowicz, and A. Claverie, Nucl. Instrum. Methods Phys. Res. B **253**, 145 (2006).
[11] F. Hüe, M. J. Hÿtch, H. Bender, F. Houdellier, and A. Claverie, Phys. Rev. Lett. **100**, 156602 (2008).
[12] F. Hüe, M. J. Hÿtch, H. Bender, J.-M. Hartmann, and A. Claverie, Mater. Res. Soc. Symp. Proc. **1026**, C20 (2008).
[13] K. Kunc, M. Balkanski, and M. A. Nusimovici, Phys. Status Solidi B **72**, 229 (1975).
[14] P. Vashishta, R. K. Kalia, A. Nakano, and J. P. Rino, J. Appl. Phys. **101**, 103515 (2007).
[15] P. C. Kelires, Phys. Rev. B **55**, 8784 (1997).
[16] H. Rücker and M. Methfessel, Phys. Rev. B **52**, 11059 (1995).
[17] J. W. Matthews, in *Dislocations in Solids*, edited by F. R. N. Nabarro (North-Holland, New York, 1979), Vol. 2, p. 471.
[18] M. L. Lee, E. A. Fitzgerald, M. T. Bulsara, M. T. Currie, and A. Lochtefeld, J. Appl. Phys. **97**, 011101 (2005).